J.Serb.Chem.Soc. 66(11–12)887–898(2001)
JSCS – 2912

UDC 66.097:546.92:66.087.3
Original scientific paper

New methods of controlled monolayer-to-multilayer deposition of Pt for designing electrocatalysts at an atomic level*

S. R. BRANKOVIĆ#, J. X. WANG and R. R. ADŽIĆ#

Materials Science and Technology Department, Brookhaven National Laboratory, Upton, New York, USA

(Received 15 June 2001)

Two new methods for monolayer-to-multileyer Pt deposition are presented. One involves Pt deposition by the replacement of an UPD metal monolayer on an electrode surface and the other the spontaneous deposition of Pt on Ru. The first method, exemplified by the replacement of a Cu monolayer on a Au(111) surface, occurs as a spontaneous irreversible redox reaction in which the Cu monolayer is oxidized by Pt cations, which are reduced and simultaneously deposited. The second method is illustrated by the deposition of Pt on a Ru(0001) surface and on carbon-supported Ru nanoparticles. This deposition takes place upon immersion of a UHV-prepared Ru(0001) crystal or Ru nanoparticles, reduced in H_2, in a solution containing $PtCl_6^{2-}$ ions. The oxidation of Ru to RuOH by a local cell mechanism appears to be coupled with Pt deposition. This method facilitates the design of active Pt-Ru catalysts with ultimately low Pt loadings. Only a quarter of a monolayer of Pt on Ru nanoparticles yields an electrocatalyst with higher activity and CO tolerance for H_2/CO oxidation than commercial Pt-Ru alloy electrocatalysts with considerably higher Pt loadings.

Keywords: electrocatalysis, H_2 electrooxidation, Pt, Ru, catalytic poisons.

INTRODUCTION

A great deal of effort has been devoted over the years to the development of fuel cell electrocatalysts with the aim of increasing their activity and reducing the noble metal catalyst loading. Currently, this research is experiencing a considerable momentum. In the late sixties, D. Dražić made a significant contribution to the pioneering efforts in the development of fuel cell catalysts[1] and fuel cell designs.[2] The most recent efforts have been focused on improving the so-called CO tolerance of Pt-Ru catalysts, *i.e.,* their activity for the oxidation of H_2 that is obtained by reforming methanol, which inevitably contains a certain concentration of CO.[3,4] Despite considerable advances in the development of these electrocatalysts, their activity and CO tolerance are still unsatisfactory and the Pt loadings are too high. In this article two new Pt deposition methods, which involve Pt deposition by replace-

* Dedicated to Professor Dragutin M. Dražić on the occasion of his 70th birthday.

Serbian Chemical Society active member.

ment of a UPD metal monolayer[5] and the spontaneous deposition of Pt on Ru,[6] are described. The latter has been used to obtain electrocatalysts with improved properties that can alleviate both the above impediments for polymer electrolyte (PEM) fuel cells that use a H_2/CO mixture from methanol reforming.[3,7]

Modification of electrocatalyts by metal monolayer deposition has been the subject of intensive research. The modification involve underpotential metal deposition (UPD),[8] spontaneous non-noble metal deposition[9] and noble metal deposition.[10,11] More recently, highly complex methods, like electron beam lithography[12] or STM tip induced metal deposition,[13,14] have been suggested. For Pt, which is the most important electrocatalyst, the initial deposition stage at room temperature commences with the immediate formation of a 3D nuclei which later evolve into 3D islands having a non-uniform size, shape and distribuion over the surface. This is the case even if the deposition process is limited to the submonolayer regime.[15] An exception is the result of Uosaki *et al.*[16] who found epitaxial growth of a Pt monolayer on Au(111) from an ordered $PtCl_6^{2-}$ anion adsorbate at a very small overpotential, which required long deposition times. Thus, the conventional electrodeposition processes are not promising for the preparation of bimetallic surfaces with controlled amounts of Pt and tailored Pt adlayer morphology. In the following, the replacement of an ordered UPD Cu adlayer on Au(111) with a more noble Pt submonolayer, as well as the spontaneous deposition of Pt on a Ru(0001) single crystal surface and on Ru nanoparticles, as methods to alleviate these problems and design electrocatalysts at the atomic level, are reported.

EXPERIMENTAL

The Ru(0001) and Au(111) single crystal 8×3 mm disks, obtained from Metal Crystals and Oxides, Cambridge, England, were polished with diamond pastes down to the 0.3 μm grade and additionally oriented to better than 0.1°. The Au(111) crystal was electropolished[17] and annealed in a hydrogen flame prior to each experiment. The Ru(0001) single crystal was prepared in ultra-high vacuum (UHV), following the standard procedure for Ru.[18] The chamber was then filled with ultra-pure Ar and the crystal was transferred from the UHV chamber into an Ar-filled glove box and immersed in the $PtCl_6^{2-}$ solution for a certain time. After removal from the solution, the crystal was throughly rinsed with 0.1 M H_2SO_4 and ultra pure water and, protected by a water drop, transferred to an electrochemical or STM cell. An annealed Pt wire was used as a pseudo-reference electrode in all the STM experiments while a standard Ag/AgCl/Cl^- and a reversible hydrogen electrode (RHE) were used for all the electrochemical experiments. STM studies were performed using a Molecular Imaging Pico STM with a 300S scanner and 300S Pico Bipotentiostat. The cell was made of Teflon and the STM tips were prepared from 80:20 Pt/Ir wire, insulated with Apiezon wax. The cell for *in situ* infrared spectro-electrochemical measurements and the optical path have been described previously.[19] A Mattson RS-10000 spectrometer and a PAR 273 potentiostat, both computer controlled, were used.

RESULTS AND DISCUSSION

Replacement of an UPD Cu monolayer by Pt

The obtained cyclic voltammogram for Cu UPD on Au(111) in 0.1 M H_2SO_4 + 0.1 M Cu^{2+} solution (Fig. 1) is in agreement with those in the literature.[20] The two peaks at about + 0.24 V and + 0.03 V *vs.* Cu/0.1 M Cu^{2+} in Fig. 1 represent potential regions where the UPD of Cu forms two ordered phases with distinct structures.[21] At a

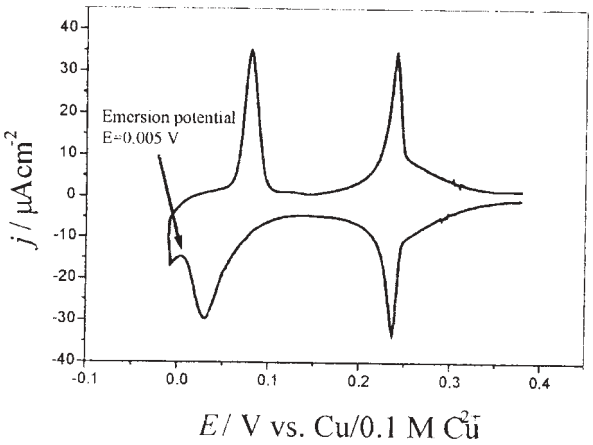

Fig. 1. Voltammetry curve for the UPD of Cu on Au(111) in 0.1 M H_2SO_4 with 0.1 M Cu^{2+}. Sweep rate 5 mV/s.

potential of 0.005 V, where the Cu adlayer has a 1×1 structure, the Au single crystal was removed from the solution into an Ar atmosphere with a preserved Cu monolayer . Then, the crystal was immersed into a solution containing 0.1 mM $PtCl_6^{2-}$ and kept in the solution for 3 min to accomplish the replacement of Cu by Pt. Finally, it was thoroughly rinsed in HNO_3 and Millipore water and, protected by a drop of water, transferred to the STM cell.

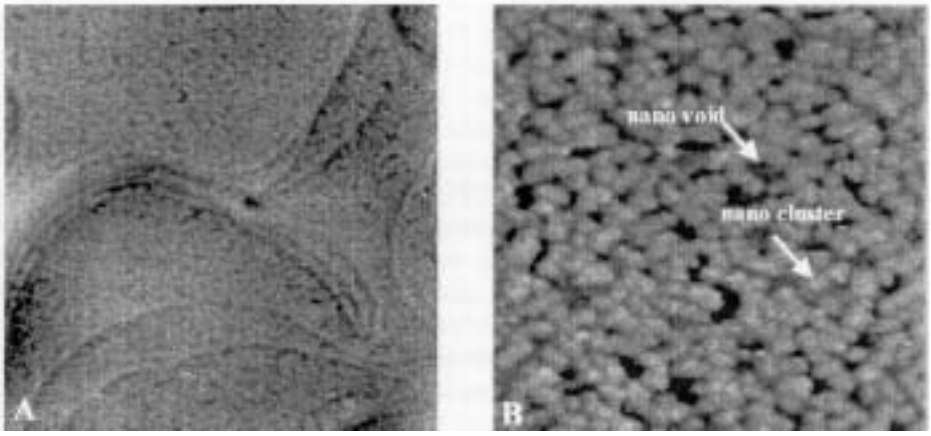

Fig. 2. STM images of a Pt submonolayer on Au(111) obtained by the replacement of a UPD Cu monolayer (see text for details). Image A: 320 × 320 nm, Z range 3 nm, image B: 105×105 nm Z range 1 nm. Images recorded in 0.1 $HClO_4$ at a potential 0.52 V *vs*. a standard Ag/AgCl/Cl^- electrode.

Figure 2 (A and B) shows two STM images of the two-dimensional Pt deposit formed on an Au(111) surface by the above procedure. Both images were obtained in 0.1 M $HClO_4$ at a potential 0.52 V *vs*. a standard Ag/AgCl/Cl^- electrode, which is positive of the UPD of Cu on Pt. Therefore, the entire deposit formed on the Au(111) surface consists of Pt metal and no residual Cu can be present on the surface. The Au(111) single crystal surface is covered by a uniform, fine, one monolayer high Pt deposit. The Pt

deposit is not formed as a continuous layer on the Au(111), surface but as a fine structure, which is better seen in image B (105 nm×105 nm) where the STM tip can resolve small 3 to 5 nm monoatomic clusters. These Pt nano-clusters are partially interconnected, but a large part of them are separated by small and narrow regions of bare Au surface ("nano-voids"). This produces an unusual, textured submonolayer deposit that uniformly covers the whole surface of the Au electrode. There is no sign of any preferential Pt deposition along step edges or on other defect sites on the Au surface, which is usually the case in electrodeposition processes.

The spontaneous deposition of Pt on a Au surface at open circuit potential is not known, so the only possibility is that the Pt deposition on Au(111) was induced by the Cu UPD adlayer in contact with the solution containing $PtCl_6^{2-}$ ions. The process occurs as a spontaneous irreversible redox reaction in which one Pt^{4+} ion from the solution oxidizes two Cu UPD adatoms, while it is simultaneously reduced to Pt^0, *viz*.,

$$2Cu^0/Au(111) + PtCl_6^{2-} \Rightarrow Pt^0/Au(111) + 2Cu^{2+} + 6Cl^- \quad (1)$$

The driving force for this reaction is the positive difference between the equilibrium potential of Pt in contact with its solvated ions and the equilibrium potential of the Cu UPD adlayer.[22,23] The amount of Pt deposited by the displacement of a full UPD monolayer of Cu is limited to a coverage of 1/2 ML because Cu oxidation can supply two electrons per adatom, while four electrons are necessary for the reduction of a Pt^{4+} ion (*cf*., Eq. (1)). Ideally, only if all of the Pt clusters were one atom high, would their coverage be an average 50 %. This is almost achieved in this case since the STM images in Fig. 2 show that, except for a few, all the Pt clusters are of monoatomic height. The uniform coverage by Pt clusters suggests that the initial nucleation of Pt is also uniform. The possible explanation for this could be that in initial stage of the redox process electrons are transferred directly from the Cu UPD adatoms to the Pt ions in the double layer through direct adatom-ion interaction. Upon reduction of the Pt ions, the Pt adatoms can diffuse over the surface to form Pt clusters or to meet other Pt adatoms and form stable nuclei. Simultaneously, the oxidized Cu adatoms dissolve and Cu^{2+} ions diffuse into the solution. The fact that the Cu UPD layer covers the Au surface uniformly means that the probability for the initial $Pt^{4+} - Cu^0$ interaction is similar over the entire surface and, consequently, a uniform formation of Pt nuclei can be expected. The large-scale image in Fig. 2 shows that this is actually achieved. An alternative procedure which facilitates a multilayer Pt deposition in this system has been described elsewhere.[5]

Spontaneous deposition of Pt on Ru(0001)

Spontaneous deposition of Pt on Ru is an unusual phenomenon, which involves a monolayer-to-multilayer deposition of one noble metal (Pt) on another noble metal (Ru). The spontaneous deposition of Pt on Ru(0001) was carried out from 10^{-2} and 10^{-4} M $[PtCl_6]^{2-}$ + 0.1 M H_2SO_4 solution. The Ru crystal was immersed in the platinum containing solution immediately after transfer from the UHV chamber to an Ar-filled glove box. The images were recorded in 0.1 M H_2SO_4 solution at a potential of 0.150 V *vs.* $AgCl/Cl^-$. The morphology of the Pt deposit on a Ru single crystal immersed in a 10^{-4} M

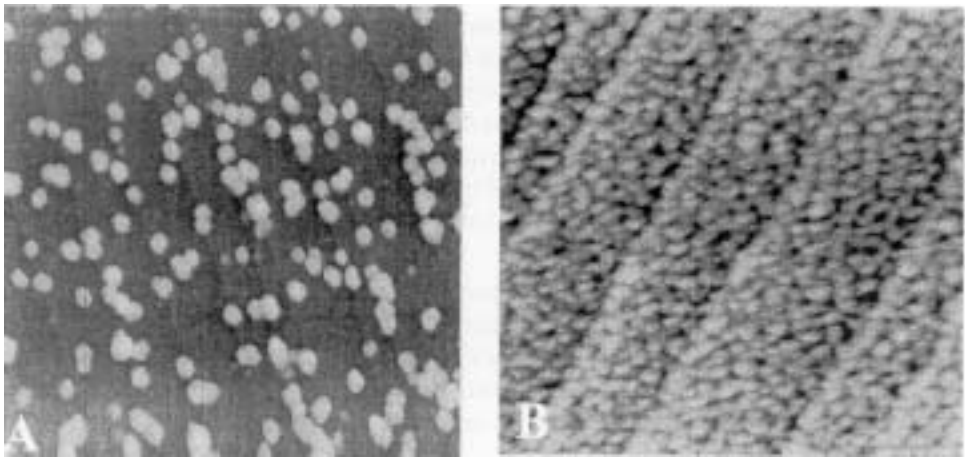

Fig. 3. STM images in H_2SO_4 solution of (A) Pt clusters spontaneously deposited on Ru(0001) in 0.1 mM H_2PtCl_6 + 0.1 M H_2SO_4 solution (see text for details), (B) Pt adlayer spontaneously deposited on Ru(0001) in 10 mM H_2PtCl_6 + 0.1 M H_2SO_4 solution (see text for details). Image A: 200×200 nm, Z range 5 nm, image B: 100×100 nm, Z range 2 nm. Images recorded at the open circuit potential in 0.1 M H_2SO_4.

$PtCl_6^{2-}$ + 0.1 M H_2SO_4 solution for 2 min is presented in Fig. 3 A. It can be seen that the Ru surface is decorated with a great number of Pt clusters, some of which were nucleated predominantly on the step edges. The Pt clusters have a column shape and relatively uniform size. Their height is in the range of 3 to 5 nm (10–15 ML) and their diameter is between 6–10 nm (Fig. 3 A). The clusters cover about 35 % of the Ru surface, as determined from the STM images. By assuming the average height of the clusters to be 4 nm (≈13 ML), it can be estimated that the total amount of Pt deposited is between 4 and 5 ML.

A representative STM image of a Pt deposit obtained by immersing a freshly prepared Ru single crystal in a 10^{-2} M $PtCl_6^{2-}$ + 0.1 M H_2SO_4 solution for one minute (half the time for the deposit in Fig. 3A) is shown in Fig. 3B. The entire Ru surface is covered with 2–6 nm-sized Pt clusters. There is an indication of a slight preferential deposition of Pt on the step edges. The average height of the Pt clusters deposited on the Ru terraces is 2 ML, while the clusters that are deposited along the step edges are in general one monolayer higher (3 ML). Since most of the Pt clusters have a very similar height and size, the morphology of underlaying Ru(0001) surface (steps and terraces) can be easily recognized (Fig. 3B). The STM images show that about 92 % of the Ru surface is covered and the total amount of deposited Pt is approximately 2 ML. Figs. 3A and 3B show that, depending on the experimental condition, Pt deposits of vastly different morphologies can be obtained on Ru(0001) surfaces.

Although the concentration of the solution in each experiment was different, a comparison of the amount of deposited Pt shows that it is proportional to the time of the crystal immersion. This was confirmed when the time was extended to 30 min in 10^{-3} M Pt solution when the amount of deposited Pt was > 10 ML.[6] It is also interesting that even though the concentration of the solution in the case of Fig. 3B was 100 times higher than in the case of Fig. 3A, the amount of Pt deposited was less since the time of

immersion was half as long. It seems that concentration, as a parameter, does not play a decisive role in determining the amount of deposited Pt. On the other hand, the morphology of the Pt deposits obtained in experiments with a shorter immersion time (Fig. 3A, 2 min. and Fig. 3B, 1 min) suggests that the density of the Pt clusters on a Ru surface is dependent on the concentration of the $PtCl_6^{2-}$ ions. The concnetration of the $PtCl_6^{2-}$ ions in Fig. 3B is two orders of magnitude higher than in Fig. 3A. This is the most probable explanation why the density of the clusters in Fig. 3B is approximately 25 times higher than in Fig. 3A.

These results indicates that the spontaneous deposition of Pt on a Ru(0001) surface when monolayer-to-multilayer deposits are formed is a different phenomenon from the spontaneous deposition of Ru or Pd on Pt as illustrated by Ru/Pt(*hkl*)[10,11] and Pd/Pt(*hkl*)[25] systems where submonolayer amounts of metal were deposited apparently through an irreversible anion adsorption, since an additional voltammetric treatment was necessary to obtain metallic deposits.

It is interesting that no spontaneous deposition of Pt occurred on a Ru(0001) surface that had been immersed in 0.1 M H_2SO_4, 0.1 M $HClO_4$ or pure H_2O for some time (1–30 min) prior to the addition of $PtCl_6^{2-}$ ions, *i.e.,* the formation of an observable Pt deposit was not detected by *in situ* STM experiments. This suggests that only a freshly UHV prepared Ru(0001) surface in contact with a $PtCl_6^{2-}$ containing electrolyte is susceptible to spontaneous Pt deposition. In addition, it also suggests that RuOH, which can form in contact with H_2O under such conditions, reduces or prevents spontaneous deposition of Pt. Our *in situ* surface X-ray scattering (SXS) and STM studies of Ru(0001) surface in acidified solution[26] showed that Ru strongly interacts with H_2O molecules even at the open circuit potential and forms an adlayer similar to RuOH. The difference between a Ru-H_2O adlayer formed in contact with H_2O at the open circuit potential and a RuOH adlayer formed by applying an oxidation potential lies only in the Ru–O interlayer separation.[26] The Ru interaction with H_2O molecules could be promoted to some form of oxidation of Ru if the immersing electrolyte contains some oxidizing species such as noble metal ions. This can account for the initial stage of the observed spontaneous deposition of Pt on Ru(0001) from $PtCl_6^{2-}$ solution. The driving force for this process, ΔU, could be the difference between the potential of $PtCl_6^{2-}$ reduction (onset of Pt deposition[16]), and the potential of Ru^0 oxidation, *viz*.,

$$\Delta U = \Delta E_{Pt^{4+}/Pt} - \Delta E_{Ru(oxidized)/Ru} > 0 \quad (2)$$

Here $\Delta E_{Ru^0 / Ru(oxidized)}$ stands for the potential of the general oxidation reaction defined by Eq. (3);

$$Ru^0 + x(H_2O) = RuO_xH_y + (2x–y)H^+ + (2x–y)e^- \quad (3)$$

It is, however, not clear to what extent the Ru oxidation reaction occurs in a spontaneous multilayer deposition of Pt. The fact that Pt can form a multilayer deposit on a Ru surface indicates that, either the oxidation of Ru to Ru(OH) is not limited to strictly one (surface) monolayer, or a higher oxidation state of Ru is formed, or some third reaction occurs. The oxidative dissolution of Ru can be excluded because it occurs at poten-

tials more positive than the equilibrium potential of $Pt/PtCl_6^{2-}$.[27] It is well known that ruthenium can easily form the oxygen containing species RuOH by reaction (3) with x, $y = 1$. The onset of this reaction on Ru(0001) in non-adsorbing acid solutions is at $E =$ 0.05 V *vs*. Ag/AgCl/Cl^-.[26] This is more negative than the equilibrium potential of $Pt/PtCl_6^{2-}$, and the condition for the spontaneous deposition of Pt defined by Eq. (2) is satisfied. *In situ* SXS and voltammetry of the oxidation of Ru(0001), however, show that oxidation beyond a monolayer of RuOH requires very high potentials above 1.2 V.[26] Therefore, further work is needed to clarify this question.

Electrocatalytic properties of Pt submonolayers on carbon supported Ru nanoparticles

The approach developed in the study of the spontaneous deposition of Pt on Ru(0001) was extended to the system where the Ru substrate was present in the shape of carbon supported nanoparticles. It was found that spontaneous deposition of Pt also occurs on Ru nanoparticles reduced in H_2 at elevated temperatures. This opens the possibility of decorating the surface of Ru nanoparticles with two-dimensional Pt clusters and thus to "tailor" the properties of the Pt/Ru bimetallic electrocatalysts on an atomic level. In addition, this approach facilitates a considerable reduction of the Pt loading by depositing Pt only at the surface of the Ru nanoparticles rather than having Pt distributed throughout the Pt-Ru nanoparticles. In contrast to Pt-Ru alloy catalysts, this structure has all the Pt atoms available for the catalytic reaction. The properties of the new Pt/Ru catalyst prepared in this way were tested and its activity compared with that of commercial Pt-Ru alloy catalysts with the same nanoparticle size.

A preparation of this Pt-Ru electrocatalyst involved the treatment of Ru (10 %) nanoparticles on Vulcan XC-72 carbon in a H_2 atmosphere at ≈300 ºC for 2 h. After cooling to room temperature, they were immersed in a solution of $PtCl_6^{2-}$ ions. The entire procedure was performed in either a H_2 or an Ar atmosphere and the amount of Pt available for spontaneous deposition was controlled by the concentration and volume of the immersing solution. The modified nanoparticles were dispersed in 100 ml of ultrapure water and sonified for 30 min. Aliquots (several μl) of a sonificated dispersion of Pt modified Ru nanoparticles were applied to a glassy carbon rotating disk electrode and covered with very thin Nafion® films.[28]

A considerable amount of work has been done on the characterization of carbon supported metal nanoparticles. The prevailing view is that they are in the form of cubo-octahedral[29] and icosohedral[30] structures. Our high-resolution transmission electron microscopy (HRTEM) data show that the Ru nanoparticles were on average 2 nm in diameter and that they grew to 2.5 nm upon deposition of Pt. A model of a cubo-octahedral Ru nanoparticle with a quarter ML of Pt and a possible distribution of the Pt clusters is given in Fig. 4.

To establich the optimal testing methodology, the mass-specific current for H_2 oxidation was measured as a function of both the Pt loading and the Nafion® film thickness by decreasing them gradually from the commonly used values.[28,31] For each sample, the current density at 50 mV was measured at 2500 rpm and normalized to the Pt

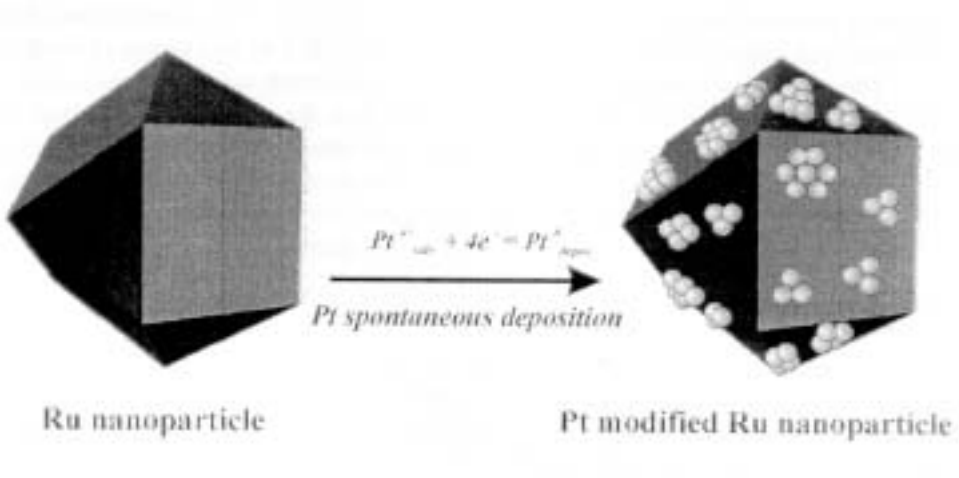

Fig. 4. Model of a cubo-octahedral Ru nanopaticle covered by a quarter of a Pt monolayer.

loading. Although there are certain statistical errors resulting mainly from the measurements of the loading and variations in the smoothness of the catalyst layer, the trend can be clearly seen in the results listed in Table I. For E-TEK Pt/Ru catalysts, the mass-specific current increases several times with decreasing Pt loading and Nafion® film thickness. The effect of the Nafion® film becomes negligible below a thickness of 10 nm. Significant irreproducibility was encountered with the electrodes with 1.95 μg/cm^2 loading. More reliable data were obtained, however, for slightly larger Pt loadings of 3 μg/cm^2 and they represent the activity of the E-TEK Pt/Ru catalyst. The results for the catalysts prepared by the spontaneous deposition of Pt with three different Pt:Ru ratios are also given in Table I. The activities are about three times those of the E-TEK Pt/Ru alloy. These data indicate that even with a low Pt coverage on Ru its activity for H_2 oxidation is preserved, which is a prerequisite for an active CO tolerant catalyst.

Figure 5 displays a comparison of the current as a function of time recorded at 2500 rpm for the oxidation of H_2 with 100 ppm of CO for the electrocatalysts $PtRu_{20}$ obtained by spontaneous deposition, and for the E-TEK Pt/Ru catalyst. The catalyst loadings are calculated with respect to the total amount of Pt and they were 0.95 and 2.93 μg/cm^2, respectively. The time dependence of the normalized current density at 50 mV shows a considerably better CO tolerance of the electrocatalyst obtained by spontaneous deposition despite the three times lower amount of Pt. The current density used for normalization was the current density for the oxidation of pure H_2, which was the same for both electrocatalysts. During the first 20 min, not shown in the graph, H_2/CO mixture was bubbled through the solution while the electrodes were subjected to the same polarization and rotation regimes as indicated in the Figure. The curves in Fig. 5 represent typical results.

The higher CO tolerance of the spontaneously deposited Pt on Ru than that of the Pt-Ru alloy electrocatalyst is likely to be a consequence of the combination of an electronic effect and the bifunctional mechanism. The latter has often been cited for the Pt-Ru system because of RuOH formation at low potentials, which helps in CO oxidation. At low

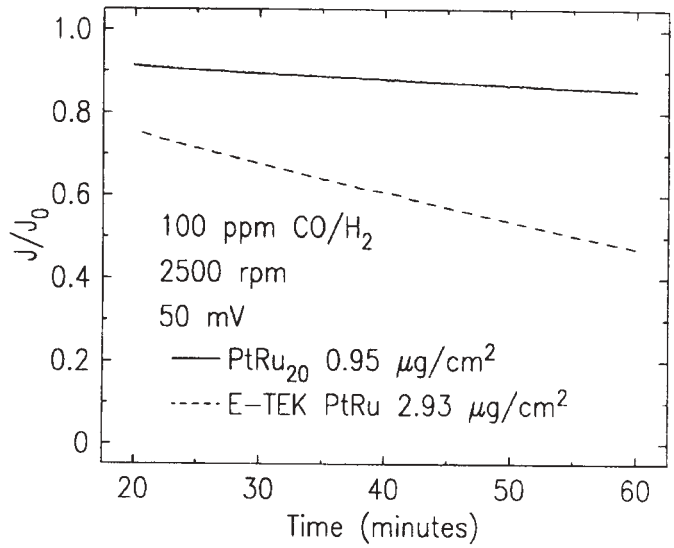

Fig. 5. Time dependence of the normalized current for the oxidation of H_2 with 100 ppm CO in 0.5 M H_2SO_4 at 25 ºC obtained using a thin-film rotating electrode at 2500 rpm; j_0 is the H_2 oxidation current. During the first 20 min the current fluctuations (not shown) are large due to the conditioning of the solution.

overpotentials, *viz*., 50–100 mV, in addition to RuOH, the Ru surface is covered by strongly adsorbed H_2O, as shown in our recent X-ray scattering study of the Ru(0001) surface.[26] Both species are probably participating in the oxidation of CO. As a consequence of the modified electronic properties of the Pt submonolayer and of the Ru substrate, the bonding of CO with Pt and Ru is expected to be weaker than with the two metals in pure phases.

TABLE I. Mass-specific current (j) measured at 50 mV at 2500 rpm for H_2 oxidation in 0.5 M H_2SO_4 at 25 ºC as a function of Pt loading and Nafion® film thickness for an E-TEK Pt-Ru electrocatalyst and the electrocatalyst Pt-Ru_x obtained by spontaneous deposition.

Sample	Pt/(nmol/cm^2)	Pt/(μg/cm^2)	D_{nafion}/(nm)	j/(A/mg)
PtRu	100	19.5	100	0.13
PtRu	25	4.88	50	0.52
PtRu	15	2.93	10	0.82
PtRu	15	2.93	5	0.86
PtRu	15	2.93	1	0.90
PtRu	10	1.95	1	1.05
$PtRu_5$	5	0.95	1	2.58
$PtRu_{10}$	5	0.95	1	2.48
$PtRu_{20}$	5	0.95	1	2.64
$PtRu_{20}$	3	0.57	1	3.74

In situ FTIR measurements of CO adsorption on Ru(0001)/Pt

The CO stretching frequency is considered to be a useful probe of the modification of surfaces to which CO is adsorbed. Fig. 6 displays SNIFTIR spectra for CO adsorbed on the submonolayer of Pt on a Ru(0001) surface as a function of potential. Two bipolar bands have potential-dependent frequencies, which change from 2011 to 2021 cm^{-1} and 2070–2073 cm^{-1}. The first band is associated with CO adsorbed on Ru(0001), but shifted to higher frequencies compared to the band between 2000 to 2013 cm^{-1} [24] for bare Ru(0001) obtained under the same conditions. The second band which lies between 2075 and 2080 cm^{-1} is due to CO adsorption on Pt and is red-shifted in comparison to the band for Pt(111).[32] This indicates a decrease of the bond strength of CO to Ru and an increase of the bond strength to Pt. The decrease in frequency of the vibration observed for Pt-Ru alloys in comparison to Pt has been interpreted as a sign of a stronger bond of CO to the alloy.[32]

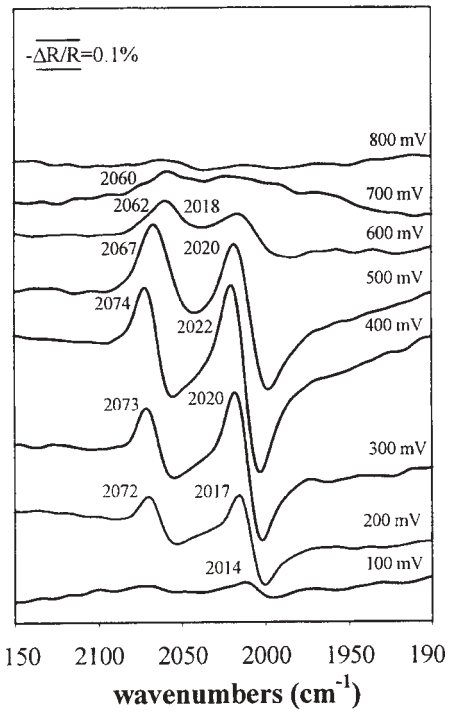

Fig. 6. SNIFTIRS spectra for a Ru(0001) electrode with a submonolayer of Pt in a CO-saturated 0.1 M H_2SO_4 solution. The reference spectrum was obtained at 0.075 V and the sample spectra were taken from 0.10 V incremented by 100 mV up to 0.80 V. 8192 scans were co-added in 16 cycles, 512 scans each; the resolution was 8 cm^{-1}. The spectra are offset for clarity.

Theoretical calculations for Ru on Pt clusters also indicate a small increase in bonding energy (decrease in frequency) and a preferential adsorption of CO on Ru.[33] The argument is based on the work function difference between Pt and Ru and the expected charge transfer from Ru to Pt which supports the increased bond strength to Pt. Therefore, the observed decrease in frequency for the CO on Pt band may not be surprising. It is, however, important that an increase of the band frequency is observed with respect to Ru (2000–2020 cm^{-1}).[24,34,35] In addition, an icrease of the

band frequency is observed if the Pt band is compared to the single band for a Pt-Ru (50:50) alloy (2055–2065 cm^{-1}), indicating a weaker bond to Pt in this electrocatalyst than with the Pt-Ru alloy. On the other hand, the temperature programmed desorption (TDS) data for CO on Pt on Ru(0001) indicate a decrease in bonding strength of CO to Pt.[36] The reasons for a difference between the IR and theoretical studies, and the TDS data are not clear at present.

CONCLUSIONS

Two new Pt deposition techniques are presented that potentially have an important application in the prepartion of fuel cell catalysts with very low Pt loadings. In addition, they facilitate studies of the cluster size effect in electrocatalysis and of the properties of bimetallic surfaces. In both cases, Pt deposition occurs as a spontaneous process yielding Pt deposits with a uniform coverage and nanometer scale morphology. An important feature of the UPD monolayer replacement method is that the deposition is a surface adlayer controlled reaction, where the amount of deposited Pt is determined by the UPD metal monolayer coverage.

The spontaneous deposition of Pt on Ru(0001) is a new phenomenon involving a noble metal deposition on a noble metal substrate. A local cell mechanism appears to be responsible for Pt deposition on Ru, where Ru oxidation to RuOH is the cathodic reaction occurring on the crystal surface. The coverage and morphology of the Pt deposit can be conveniently controlled by the time of crystal immersion and concentration of $PtCl_6^{2-}$ ions. The electrocatalysts prepared by the spontaneous deposition of Pt on Ru nanoparticles have high activity and high CO tolerance exceeding those of the state-of-the-art commercial catalysts containing several times higher Pt loadings.

Acnowledgments: This work was supported by the U. S. Department of Energy, Divisions of Chemical and Material Sciences, under the Contract No. DE-AC02-98CH10886. The authors thank S. Feldberg, J. McBreen and N. Marinković for useful discussions.

И З В О Д

НОВИ МЕТОДИ ЗА КОНТРОЛИСАНУ МОНОСЛОЈНО И МУЛТИСЛОЈНО ТАЛОЖЕЊЕ Pt ЗА ДИЗАЈН КАТАЛИЗАТОРА НА АТОМСКОМ НИВОУ

СТАНКО Р. БРАНКОВИЋ, J. X. WANG и РАДОСЛАВ Р. АЦИЋ

Materials Science and Technology Department, Brookhaven National Laboratory, Upton, New York, USA

У овом раду су презентована два нова метода за контролисано монослојно и мултислојно таложење Pt. Први метод је базиран на замени монослојева метала таложених на потпотенцијалима и дат је на примеру замене Cu монослоја на Au(111) са парцијалним монослојем платине. Други метод је базиран на новом феномену спонтаног таложења Pt на металну површину Ru. По првом методу Cu монослој се оксидише јонима Pt који се истовремено редукују и таложе на површину злата. Спонтано таложење Pt на Ru се дешава кад се Ru кристал припремљен у високом вакууму, или Ru наночестице редуковане у H_2 на повишеној температуре, унесу у раствор који садржи H_2PtCl_6. Таложење се одвија по механизму локалне галванске ћелије уз оксидацију Ru

до RuOH која се одвија на површини електроде. Овај метод пружа значајну погодност за дизајн Pt/Ru катализатора са веома малом количином Pt. Ru наночестице са степеном покривености од само 1/4 монослоја Pt показују значајно побољшану толеранцију према CO и већу активност за оксидацију H_2 у поређењу са најбољим комерцијалним Pt-Ru катализаторима.

(Примљено 15. јуна 2001)

REFERENCES

1. D. M. Dražić, R. R. Adžić, *Electrochim. Acta* **14** (1965) 5
2. D. M. Dražić, R. R. Adžić, A. R. Despić, *J. Electrochem. Soc.* **116** (1969) 885
3. S. Gottesfeld, T. A. Zawodzinski, in *Advances in Electrochemical Science and Engineering,* Vol. 5, R. C. Alkire, D. M. Kolb, Eds., Wiley - VCH, Weinham, 1997
4. N. M. Marković, P. N. Ross, *Electrochim. Acta* **45** (2000) 4101
5. S. Branković, J. Wang, R. R. Adžić, *Surf. Sci.* **470** (2001) L173
6. S. R. Branković, J. McBreen, R. R. Adžić, *J. Electroanal. Chem.* **503** (2001) 99
7. H. A. Gasteiger, N. Marković, P. N. Ross, E. J. Cairns, *J. Phys. Chem.* **97** (1993) 12020
8. R. R. Adžić, in *Adv. Electrochem. & Electrochem. Eng.,* Vol. 13, H. Gerisher Ed., Wiley, N. Y., 1984
9. M. M. P. Jansenn, J. Moolhuysen, *Electrochim. Acta* **21** (1976) 861
10. W. Chrzanowski, A. Wieckowski, *Langmuir* **13** (1997) 5974
11. E. Herrero, J. M. Feliu, A. Wieckowski, *Langmuir* **15** (1999) 4944
12. P. W. Jacobs, S. J. Wind, F. H. Ribeiro, G. A. Somorjai, *Surf. Sci.* **372** (1997) L249
13. D. M. Kolb, R. Ulmann, T. Will, *Science* **275** (1997) 1097
14. J. V. Zoval, R. M. Stiger, P. R. Beirnacki, R. M. Penner, *J. Phys Chem.* **100** (1996) 837
15. H. F. Waibel, M. Kleinert, D. M. Kolb, *Electrochem. Soc. Meeting Abstract*, 354, Spring 2001
16. K. Uosaki, S. Y. Hideo, Y. Oda, T. Haba, T. Kondo, *J. Phys. Chem. B* **101** (1997) 7566
17. K. Sieradzki, S. R. Branković, N. Dimitrov, *Science* **284** (1999) 138
18. T. E. Madey, H. A. Engelhardt, D. Menzel, *Surf. Sci.* **48** (1975) 304
19. N. S. Marinković, M. Hecht, J. S. Loring, W. R. Fawcett, *Electrochim. Acta* **4** (1996) 641
20. Y. Nakai, M. S. Zei, D. M. Kolb, G. Lempful, *Ber. Bunsenges, Phys, Chem.* **88** (1984) 340
21. M. F. Toney, J. N. Howard, J. Richer, G. L. Borges, J. G. Gordon, O. R. Merloy, D. Yee, L. B. Sorensen, *Phys. Rev. Lett.* **75** (1995) 4472
22. S. Swathriajan, S. Burckenstein, *Electrochim. Acta* **28** (1983) 865
23. E. Schmidt, N. Wuthrich, *J. Electroanal. Chem.* **28** (1970) 349
24. N. S. Marinković, J. X. Wang, H. Zajonz, R. R. Adžić, *Electrochem. Solid-State Lett.* **3** (2000) 11
25. J. Clavilier, J. M. Feliu, A. Aldaz, *J. Electroanal. Chem.* **243** (1988) 419
26. J. X. Wang, N. S. Marinković, H. Zajonz, B. M. Ocko, R. R. Adžić, *J. Phys. Chem.* **105** (2001) 2809
27. D. Michell, D. A. J. Rand, R. Woods, *J. Electroanal. Chem.* **89** (1978) 11
28. T. J. Smith, H. A. Gasteiger, G. D. Stäb, P. M. Urban, D. M. Kolb, R. J. Behm, *J. Electrochem. Soc.* **145** (1998) 2354
29. K. Kinoshita, in *Modern Aspects of Electrochemistry*, Vol. 14, J. O'M. Bockris, B. E. Conway, R. E. White, Eds., New York, Plenum Press, 1982
30. R. E. Benfield, *J. Chem. Soc. Faraday Trans.* **88** (1992) 1107
31. S. Lj. Gojković, S. K. Zecević, R. F. Savinel, *J. Electrochem. Soc.* **145** (1998) 3713
32. W. F. Lin, M. S. Zei, M. Eiswirth, G. Ertl, T. Iwasita, W. Vielstich, *J. Phys. Chem.* **103** (1999) 6968
33. M-S. Liao, C. R. Cabrera, Y. Ishikawa, *Surf. Sci.* **445** (2000) 267
34. W. F. Lin, T. Iwasita, W. Vielstich, *J. Phys. Chem.* **103** (1999) 3250
35. W. F. Lin, P. A. Christensen, A. Hamnet, M. S. Zei, G. Ertl, *J. Phys. Chem.* **104** (2000) 6642
36. F. Buatier de Mongeot, M. Scherer, B. Gleich, E. Kopatzki, R. J. Behm, *Surf. Sci.* **411** (1998) 249.